Inorg. Chem. **2008**, *47*, 1087–1095

Counterions Influence Reactivity of Metal Ions with Cysteinyldopa Model Compounds

Yohannes T. Tesema, David M. Pham, and Katherine J. Franz*

Department of Chemistry, Duke University, Box 90346, Durham, North Carolina 27708

Received September 24, 2007

Cysteinyldopas are naturally occurring conjugates of cysteine and dopa (3,4-dihydroxy-L-phenylalanine) that are precursors to red pheomelanin pigments. Metal ions are known to influence pheomelanogenesis in vitro and may be regulatory factors in vivo. Cydo (3-[(2-amino-ethyl)sulfanyl]-4,6-di-*tert*-butylbenzene-1,2-diol) and CarboxyCydo (2-amino-3-(4,6-di-*tert*-butyl-2,3-dihydroxyphenylsulfanyl)-propionic acid) are model compounds of cysteinyldopa that retain its metal-binding functionalities but cannot polymerize due to the presence of blocking *tert*-butyl groups. Cydo reacts readily with zinc(II) acetate or nickel(II) acetate to form a cyclized 1,4-benzothiazine (zine) intermediate that undergoes ring contraction to form benzothiazole (zole) unless it is stabilized by coordination to a metal ion. The crystal structure of [Ni(zine)$_2$] is reported. The acetate counteranion is required for the zinc-promoted reactivity, as neither zinc(II) sulfate nor zinc(II) chloride alone promotes the transformation. The counterion is less important for redox-active copper and iron, which both readily promote the oxidation of Cydo to zine and zole species; Cu(II) complexes of both zine and zole have been characterized by X-ray crystallography. In the case of CarboxyCydo, a 3-carboxy-1,4-benzothiazine intermediate decarboxylates to form [Cu(zine)$_2$] under basic conditions, but in the absence of base forms a mixture of products that includes the carboxylated dimer 2,2′-bibenzothiazine (bi-zine). These products are consistent with species implicated in the pheomelanogenesis biosynthetic pathway and emphasize how metal ions, their counteranions, and reaction conditions can alter pheomelanin product distribution.

Introduction

Pheomelanins, the reddish pigments found in hair and bird feathers, are highly heterogeneous polymers and mixtures of oligomers. On the basis of degradation studies of natural pigments combined with in vitro biosynthetic studies, the major structural components of this complex pigment are benzothiazine and benzothiazole units linked in an array of possible arrangements, one example of which is shown in Chart 1.[1] In addition to these C−O and C−C couplings that lead to large polymers, lower molecular weight species termed trichochromes have also been identified as red hair pigments. The trichochromes are generally composed of benzothiazine-type dimers linked at the 2 positions, as shown in Chart 1 for trichochrome C. Some controversy persists as to whether this exact chemical structure exists in the natural pigment or is a product of isolation procedures.[2] Regardless, it is well accepted that the precursors to these red pigments are cysteinyldopas, which arise from the nucleophilic addition of cysteine to dopaquinone, itself a product of either tyrosinase oxidation of tyrosine or oxidation of dopamine.[3]

Chart 1

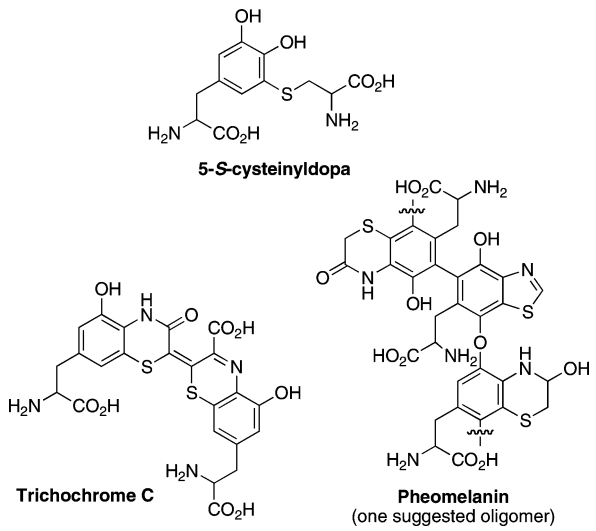

* To whom correspondence should be addressed. E-mail: katherine.franz@duke.edu.

(1) Di Donato, P.; Napolitano, A.; Prota, G. *Biochim. Biophys. Acta* **2002**, *1571*, 157−166.
(2) Di Donato, P.; Napolitano, A. *Pigment Cell Res.* **2003**, *16*, 532−539.

10.1021/ic701889w CCC: $40.75
Published on Web 12/29/2007

The importance of understanding the chemistry of cysteinyldopa is highlighted by its presence but unknown role in human diseases including melanoma and Parkinson's disease. In melanoma, the serum level of 5-*S*-cysteinyldopa, the major isomer, is a sensitive and specific marker for predicting metastases.[4] In Parkinson's disease, it has been hypothesized that the formation of cysteinyldopas diverts the normal pathway of dopamine oxidation that forms neuromelanin,[5] the pigment that darkens dopaminergic neurons in the substantia nigra that degrade during disease progression.[6,7] Although the role of neuromelanin in the disease remains elusive, benzothiazines may contribute to neurodegeneration by inhibiting key enzymes such as mitochondrial complex I,[8−10] α-ketoglutarate dehydrogenase,[11] and pyruvate dehydrogenase.[12] In addition, both cysteinyldopa and the corresponding cyclized benzothiazines are more easily oxidized than the neurotransmitter itself,[8,13] leading to speculation that oxidative processes related to these species may contribute to cell death, as has been shown in neuronal cell culture.[14,15] Metal ions, which are known to accumulate in neuromelanin, catalyze these oxidative processes.[16,17]

Extensive biosynthetic studies have revealed that the assembly of pheomelanin and trichochrome pigments from cysteinyldopas varies widely depending on reaction conditions.[2] The variables include the choice of oxidant system (for example, tyrosinase, peroxidase/H_2O_2, air, ferricyanide, or other chemical oxidants), pH, and the presence of metal ions such as zinc,[18,19] iron,[1,16] copper,[1] and others.[16,19] The role of metal ions is particularly intriguing given the evidence that magnesium, calcium, iron, copper, and zinc accumulate in human hair melanosomes,[20] and iron in particular accumulates in neuromelanin.[21−23] It has been proposed that these metal ions may act as regulatory factors in the production of pheomelanins, perhaps giving rise to their chemical variety.[1] It has even been suggested that dietary mineral nutrients including calcium, zinc, and iron impact melanin production in bird feathers.[24,25]

Chart 2

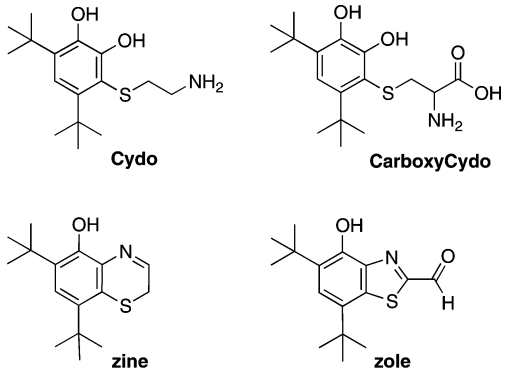

We have been interested in exploring the coordination chemistry provided by the variety of potential metal binding sites found in melanins and their precursors.[26,27] Cysteinyldopa itself contains a dihydroxy catechol unit as well as carboxylic acid, amine, and thioether functionalities, while benzothiazine and benzothiazole contain N/O bidentate chelating units. We recently introduced 3-[(2-amino-ethyl)-sulfanyl]-4,6-di-*tert*-butylbenzene-1,2-diol (Cydo) as a model of cysteinyldopa and reported the first structurally characterized examples of a metal ion, in this case Cu^{II}, coordinated by aminothioether-appended catechol and by benzothiazine.[26] In the present report, we extend these studies to investigate the reactions of Cydo with Zn^{II}, Ni^{II}, and Fe^{III} and introduce a modification of Cydo that incorporates a carboxylic acid to better model cysteinyldopa. The chemical structures of Cydo and CarboxyCydo are shown in Chart 2 together with the ring-closed benzothiazine (zine) and benzothiazole (zole) products.

Experimental Section

General Considerations. All reagents and solvents were purchased from commercial sources and used as received. Triethylamine was distilled from calcium hydride. Cydo (3-[(2-aminoethyl)-sulfanyl]-4,6-di-*tert*-butylbenzene-1,2-diol hydrochloride) and zole (5,7-di-(*tert*-butyl)-4-hydroxyl-1,3-benzothiazole-2-carbaldehyde) were prepared as described previously.[26] UV−vis spectrophotometric titrations were recorded on a Photonics model 420 fiber optic CCD array spectrophotometer by dipping a Photonics dual-source fiber optic dip probe into the titration vessel. NMR spectra were recorded on Varian Mercury 300 or Inova 400 or 500 spectrometers;

(3) Ito, S. *Pigment Cell Res.* **2003**, *16*, 230−236.
(4) Wakamatsu, K.; Kageshita, T.; Furue, M.; Hatta, N.; Kiyohara, Y.; Nakayama, J.; Ono, T.; Saida, T.; Takata, M.; Tsuchida, T.; Uhara, H.; Yamamoto, A.; Yamazaki, N.; Naito, A.; Ito, S. *Melanoma Res.* **2002**, *12*, 245−253.
(5) Shen, X. M.; Xia, B.; Wrona, M. Z.; Dryhurst, G. *Chem. Res. Toxicol.* **1996**, *9*, 1117−1126.
(6) Fedorow, H.; Tribl, F.; Halliday, G.; Gerlach, M.; Riederer, P.; Double, K. L. *Prog. Neurobiol.* **2005**, *75*, 109−124.
(7) Zucca, F. A.; Giaveri, G.; Gallorini, M.; Albertini, A.; Toscani, M.; Pezzoli, G.; Lucius, R.; Wilms, H.; Sulzer, D.; Ito, S.; Wakamatsu, K.; Zecca, L. *Pigment Cell Res.* **2004**, *17*, 610−617.
(8) Shen, X. M.; Zhang, F.; Dryhurst, G. *Chem. Res. Toxicol.* **1997**, *10*, 147−155.
(9) Li, H.; Shen, X. M.; Dryhurst, G. *J. Neurochem.* **1998**, *71*, 2049−2062.
(10) Li, H.; Dryhurst, G. *J. Neurochem.* **1997**, *69*, 1530−1541.
(11) Shen, X. M.; Li, H.; Dryhurst, G. *J. Neural Transm.* **2000**, *107*, 959−978.
(12) Li, H.; Dryhurst, G. *J. Neural Transm.* **2001**, *108*, 1363−1374.
(13) Picklo, M. J.; Amarnath, V.; Graham, D. G.; Montine, T. J. *Free Radical Biol. Med.* **1999**, *27*, 271−277.
(14) Montine, T. J.; Amarnath, V.; Picklo, M. J.; Sidell, K. R.; Zhang, J.; Graham, D. G. *Drug Metabolism Rev.* **2000**, *32*, 363−376.
(15) Spencer, J. P. E.; Whiteman, M.; Jenner, P.; Halliwell, B. *J. Neurochem.* **2002**, *81*, 122−129.
(16) Shen, X.-M.; Dryhurst, G. *Chem. Res. Toxicol.* **1998**, *11*, 824−837.
(17) Meyskens, F. L. J.; Farmer, P.; Fruehauf, J. P. *Pigment Cell Res.* **2001**, *14*, 148−154.
(18) Napolitano, A.; Di Donato, P.; Prota, G. *J. Org. Chem.* **2001**, *66*, 6958−6966.
(19) Palumbo, A.; Nardi, G.; Dischia, M.; Misuraca, G.; Prota, G. *Gen. Pharmacol.* **1983**, *14*, 253−257.
(20) Liu, Y.; Hong, L.; Wakamatsu, K.; Ito, S.; Adhyaru, B. B.; Cheng, C. Y.; Bowers, C. R.; Simon, J. D. *Photochem. Photobiol.* **2005**, *81*, 510−516.
(21) Zecca, L.; Pietra, R.; Goj, C.; Mecacci, C.; Radice, D.; Sabbioni, E. *J. Neurochem.* **1994**, *62*, 1097−1101.
(22) Zecca, L.; Tampellini, D.; Gatti, A.; Crippa, R.; Eisner, M.; Sulzer, D.; Ito, S.; Fariello, R.; Gallorini, M. *J. Neural Transm.* **2002**, *109*, 663−672.
(23) Zecca, L.; Zucca, F. A.; Toscani, M.; Adorni, F.; Giaveri, G.; Rizzio, E.; Gallorini, M. *J. Radioanal. Nucl. Chem.* **2005**, *263*, 733−737.
(24) McGraw, K. J. *Behavioral Ecol.* **2007**, *18*, 137−142.
(25) McGraw, K. J. *Oikos* **2003**, *102*, 402−406.
(26) Tesema, Y. T.; Pham, D. M.; Franz, K. J. *Inorg. Chem.* **2006**, *45*, 6102−6104.
(27) Charkoudian, L. K.; Franz, K. J. *Inorg. Chem.* **2006**, *45*, 3657−3664.

δ values are in ppm, and J values are in Hz. IR Spectra were recorded on a Nicolet 360 FT-IR. Electrospray ionization mass spectrometry (ESI-MS) was performed on an Agilent 1100 Series LC/MSD Trap Spectrometer with a Daly conversion dynode detector. Samples were infused via a Harvard Apparatus syringe pump at 33 μL/min. Ionization was achieved in the positive or negative ion mode by the application of +5 or −5 kV at the entrance of the capillary; the pressure of the nebulizer gas was 20 psi. The drying gas was heated to 325 °C at a flow of 7L/min. Full-scan mass spectra were recorded in the mass/charge (m/z) range of 50−2000. Elemental analysis was performed by Desert Analytics (Tucson, AZ).

CarboxyCydo: 2-Amino-3-(4,6-di-*tert*-butyl-2,3-dihydroxyphenylsulfanyl)-propionic Acid. A 50 mL solution of 3,5-di-*tert*-butyl-*o*-benzoquinone (1.0 g, 4.54 mmol) in methanol was added dropwise over 6 h to a stirred solution of L-cysteine (1.79 g, 13.36 mmol) in 50 mL of methanol/0.2 N HCl (1:1 v/v) to provide a colorless reaction mixture with some white precipitate. The volume was concentrated under reduced pressure to 25 mL, and the resulting white solid was collected by filtration, washed with diethyl ether (4 × 10 mL), and air-dried to give 1.3 g (84% yield) of white powder. ESI-MS: m/z 342 $[M + H]^+$. Anal. Calcd for $C_{17}H_{27}NO_4S$: C, 57.55; H, 8.45; N, 4.19. Found: C, 56.19; H, 8.67; N, 4.24. ^{1}H NMR (CD_3OD): δ 1.2 (18H, d, *t*-butyl), 3.1 (2H, d, $-SCH_2$), 3.81 (1H, t, -$CHNH_2$), and 6.9 (1H, s, aromatic). UV−vis (MeOH): 293 nm (1.91×10^3 M^{-1} cm^{-1}). IR (cm^{-1}): 3309 (m), 2954 (s), 1625 (s), 1480 (w), 1392 (m), and 1232 (m).

[Ni(zine)$_2$]. A solution of Et_3N (329 μL, 2.34 mmol) in 10 mL of methanol was added slowly to a stirred solution of $Ni(CH_3CO_2)_2 \cdot 4H_2O$ (195 mg, 0.78 mmol) and Cydo (261 mg, 0.78 mmol) in 20 mL of methanol to afford a brown precipitate almost immediately upon mixing. The precipitate was collected by filtration and washed with cold methanol (2 × 10 mL) and dried under vacuum. Single brown crystals suitable for X-ray structure determination were grown by the slow diffusion of methanol into a THF solution of the complex: yield, 161 mg (67%). Anal. Calcd for $C_{32}H_{44}N_2O_2S_2Ni$: C, 62.85; H, 7.25; N, 4.58. Found: C, 62.82; H, 7.00; N, 4.78. UV−vis (THF): 336 nm (2.4×10^3 M^{-1} cm^{-1}), 460 nm (1.1×10^3 M^{-1} cm^{-1}).

[Cu(CH$_3$OH)(zole$_{ac}$)$_2$]. A 10 mL solution of $CuCl_2 \cdot 2H_2O$ (39 mg, 0.23 mmol) in methanol was added dropwise to a stirring solution of zole (131 mg, 0.45 mmol) in 20 mL of methanol. Brown precipitate began to form upon the addition of a dilute solution of Et_3N (64 μL, 0.45 mmol) in 5 mL of methanol to the reaction mixture. The reaction mixture was stirred at room temperature for an additional 10 min, after which time the brown precipitate was isolated by vacuum filtration and washed with 2 portions of cold methanol. The product was crystallized by vapor diffusion of methanol into a concentrated THF solution of the crude brown precipitate (120 mg, 70% yield). Dark brown prismatic crystals were harvested for single-crystal X-ray structure determination. Anal. Calcd for $C_{37}H_{56}CuN_2O_7S_2$: C, 57.90; H, 7.22; N, 3.65. Found: C, 57.98; H, 6.85; N, 3.58. UV−vis (THF): 254 nm (3.7×10^4 M^{-1} cm^{-1}), 305 nm (6.0×10^3 M^{-1} cm^{-1}), 382 nm (5.5×10^3 M^{-1} cm^{-1}). IR (cm^{-1}): 2950 (m), 1474 (m), 1363 (m), 1294 (m), 1251 (m), 1194 (s), and 1070 (s). While the presence of methanol as a reaction solvent results in the conversion of the aldehyde functionality of zole to the methyl acetal functionality of zole$_{ac}$, reactions carried out in acetonitrile retain the aldehyde version of zole and yield purple prismatic crystals of $[Cu(THF)_2(zole)_2]$ suitable for single-crystal X-ray diffraction by slow evaporation of a saturated THF solution (see the Supporting Information).

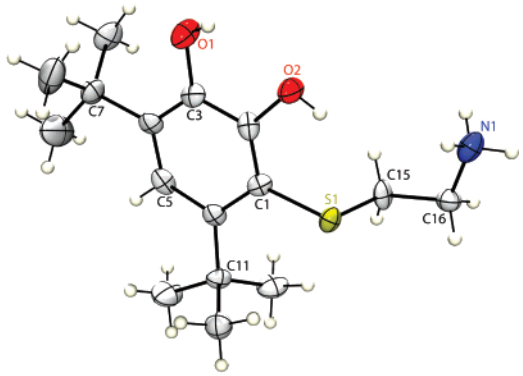

Figure 1. X-ray structure of Cydo showing 50% thermal ellipsoids. Selected bond distances (Å): S1−C1, 1.777(7); S1−C(15), 1.814(7); O2−C2, 1.370(8); C15−C16, 1.508(9); N1−C16, 1.490(9); C2−C1, 1.375(10); C4−C3, 1.356(10); C4−C7, 1.540(10); C3−O1, 1.388(8). Selected bond angles (deg): C1−S1−C15, 103.5(3); O2−C2−C1, 123.8(6); O2−C2−C3, 113.87; C1−C2−C3, 122.5(7); C10−C7−C4, 111.4(7); N1−C16−C15, 112.5(6).

X-ray Data Collection, Solution, and Refinement. All diffraction experiments were performed on a Bruker Kappa Apex II CCD diffractometer equipped with a graphite monochromator and a Mo Kα fine-focus sealed tube (λ= 0.71073 Å) operated at 1.75 kW power (50 kV, 35 mA). The detector was placed at a distance of 5.010 cm from the crystal. Each data set was collected with a total of 1548 frames with a scan width of 0.5°. Exposure times for each experiment were dependent on the diffraction intensity of each sample. The frames were integrated with the Bruker *SAINT*, version 7.12A, software package using a narrow-frame integration algorithm. Empirical absorption corrections were applied using *SADABS*, version 2.10, and the structure was checked for higher symmetry with *PLATON*, version 1.07. The structures were solved by direct methods with refinement by full-matrix least squares based on F^2 using the Bruker *SHELXTL* software package. All non-hydrogen atoms were refined anisotropically, with the exception of disordered solvent molecules and minor disordered components. Hydrogen atoms of sp^2 hybridized carbons and nitrogens were located directly from the difference Fourier maps; all others were calculated.

The best quality crystal found for the $[Ni(Zine)_2]$ complex was a non-merohedral twinned crystal with two primary orientations rotated 180° from each other. The orientation matrices of the two domains were computationally determined by the program *CELL_NOW*,[28] and their occupancies were refined to be roughly equal (52.1% ∼ 47.9%). The $[Cu(CH_3OH)(zole_{ac})_2]$ structure contains a disordered methyl site at one of the four acetal groups, which was modeled with C9a and C9b. This disorder arises from the pivoting of the O2−C8 bond, which smears the electron density across the C9a/b positions. The occupancies at these two sites were refined to be roughly equal (45.7 and 54.3%).

Results

Reactivity of Cydo with Zinc(II) and Nickel(II) Acetate. The ligand Cydo (see Chart 2) was introduced as a model of cysteinyldopa that contains catechol, thioether, and amine functionalities but also has *t*-butyl groups at the C4 and C6 positions that prohibit the polymerization of its reaction products. These positions were blocked in order to avoid making complex mixtures of pheomelanin-type oligomers such as the one shown in Chart 1, while focusing on metal

(28) Sheldrick, G. *Cell_Now*; Bruker-AXS, Inc.: Madison, WI, 2004.

Table 1. Summary of X-ray Diffraction Parameters

	[Cydo·HCl]·H_2O	(bi-zine)·Et_2O ·2(H_2O)	[Ni(zine)$_2$]	[Cu(CH_3OH)(zole$_{ac}$)$_2$]
formula	$C_{32}H_{60}Cl_2N_2O_6S_2$	$C_{36}H_{46}N_2O_{7.5}S_2$	$C_{32}H_{44}N_2NiO_2S_2$	$C_{37}H_{56}CuN_2O_7S_2$
fw	703.84	690.87	611.52	767.49
a, Å	6.0792(8)	35.489(4)	12.6926(7)	12.4207(4)
b, Å	18.230(2)	10.401(1)	8.9361(5)	12.6635(4)
c, Å	18.637(3)	21.616(2)	14.6865(7)	25.5745(8)
α, deg	106.234(3)	90	90	90
β, deg	95.310(3)	107.672(2)	108.518(3)	98.852(2)
γ, deg	91.169(3)	90	90	90
V, Å^3	1972.2(5)	7602(1)	1579.5(2)	3974.7(2)
Z	2	8	2	4
cryst syst	triclinic	monoclinic	monoclinic	monoclinic
space group	$P\bar{1}$	*C*2/*c*	$P2_1/c$	$P2_1/n$
T, K	298(2)	298(2)	173(2)	298(2)
λ, Å	0.71073	0.71073	0.71073	0.71073
ρ, g/cm^3	1.185	1.207	1.286	1.283
μ, mm^{-1}	0.310	0.188	0.777	0.701
R_1 (obsd data)	0.0737	0.0850	0.0376	0.0397
R_2 (all data, F^2 refinement)	0.2062	0.2591	0.1099	0.1209

complexes that correspond to species early in the pheomelanogenesis pathway. A single X-ray-quality crystal of Cydo was obtained by the slow diffusion of diethyl ether into a methanol solution of the compound. The structure with the atom numbering scheme of the ligand is shown in Figure 1 together with selected bond distances and angles. Table 1 contains a summary of the crystallographic data for all of the structures reported here.

The reactivity of Cydo with Zn^{II}, Ni^{II}, and Fe^{III} was investigated and followed spectrophotometrically by titrating methanol solutions of Cydo with methanol solutions of the metal salts in air at ambient room temperature. Figure 2 shows the UV−vis spectra that appear upon the titration of Cydo with zinc(II) acetate. The characteristic absorption band at 293 nm due to Cydo diminishes, and an intense absorption band at 310 nm increases, accompanied by an isosbestic point at 300 nm. The absorption maximum at 310 nm is consistent with the formation of 1,4-benzothiazine (abbreviated here as zine), a species known to result from the intramolecular condensation of cysteinyldopa or its analogues upon oxidation.[18,19,29] The signature peak maximizes after 1 equiv of Zn^{II} (and the corresponding 2 equiv of acetate) has been added. The colorless solution turns a very pale yellow over the course of the titration, but becomes bright yellow after ∼12 h to give the final spectrum shown in Figure 2B with $\lambda_{max} = 410$ nm. This spectroscopic signature is indicative of 4-hydroxy benzothiazole (abbreviated here as zole), a product of ring contraction from benzothiazine.[26]

ESI-MS analysis of the reaction mixture confirmed the presence of both zine ($m/z = 278$) and the acetal derivative of zole$_{ac}$ (5,7-di-*tert*-butyl-2-dimethoxybenzothiazol-4-ol, $m/z = 338$) as the two major products (the acetal forms when the aldehyde version of zole is exposed to methanol).

As shown by the spectra in Figure 3, several similarities are observed when 1 equiv of nickel(II) acetate is added in place of zinc(II) acetate to a methanol solution of Cydo. The characteristic absorption band of Cydo at 293 nm diminishes with a gradual shift to an intense absorption band at 310 nm accompanied by an isosbestic point at 300 nm. Unlike the Zn case in which the solution turns bright yellow over 12 h, a dark brown precipitate forms over the course of a few hours in the Ni case. The dark brown precipitate was isolated and crystallized from THF by the slow diffusion of methanol to yield a mononuclear nickel complex [Ni(zine)$_2$]. The yield of [Ni(zine)$_2$] was increased substantially when Et_3N was added to the reaction mixture.

X-ray-quality crystals of [Ni(zine)$_2$] were obtained by the slow diffusion of methanol into a THF solution of the complex. The crystal structure of [Ni(zine)$_2$] is depicted in Figure 4, and selected bond distances and angles are listed in the figure caption. The asymmetric unit consists of a zine unit coordinated via a phenolate O and imine N to Ni^{II}, which sits on a crystallographic inversion center that generates the square-planar N_2O_2 coordination environment around Ni. The structure is very similar to that of a Cu^{II} analogue we previously reported.[26] The 1.885(2) Å Ni−N and 1.846(2) Å Ni−O bond distances are typical of Ni^{II}−N(imine) and Ni^{II}−O(phenolate) bonds,[30] but are slightly shorter than the Cu^{II}−N(imine) (1.964(2) Å) and Cu^{II}−O(phenolate) (1.894(5) Å) bond distances found in the copper version [Cu(zine)$_2$].[26]

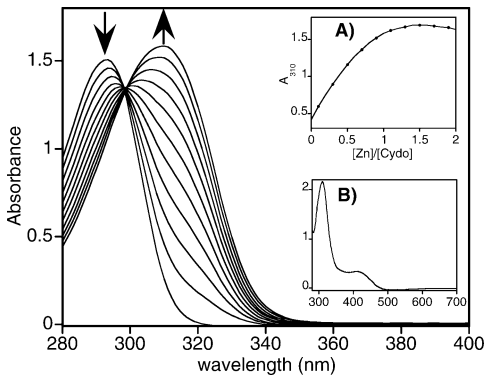

Figure 2. UV-spectrophotometric titration of 0.57 mM Cydo with Zn(CH_3CO_2)$_2$·2H_2O in methanol at room temperature. Inset A shows that the band at 310 nm plateaus after the addition of 1 equiv of Zn^{II}. Inset B displays the spectrum of the reaction mixture after 12 h. The peak at 410 nm indicates the presence of a benzothiazole product.

(29) Napolitano, A.; Di Donato, P.; Prota, G.; Land, E. J. *Free Radical Biol. Med.* **1999**, *27*, 521−528.

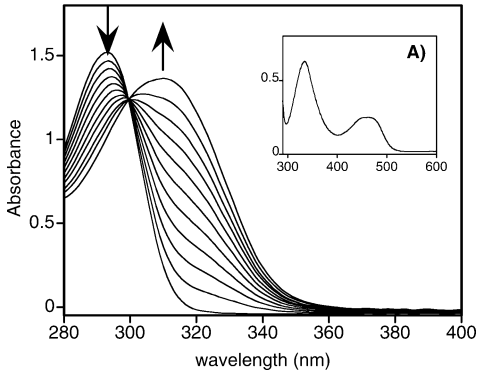

Figure 3. UV-spectrophotometric titration of 0.57 mM Cydo with 1 equiv of $Ni(CH_3CO_2)_2 \cdot 4H_2O$ in methanol at 25 °C. Inset A shows the UV−vis spectrum of $Ni(zine)_2$ in THF.

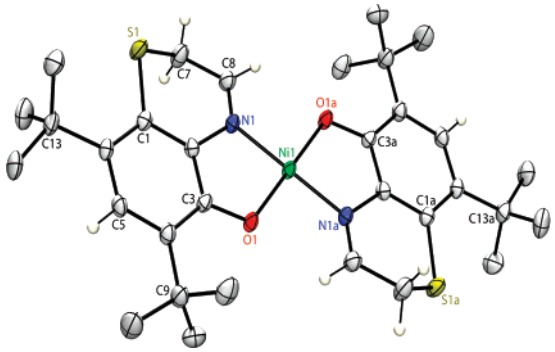

Figure 4. X−ray structure of $Ni(zine)_2$ showing 50% thermal ellipsoids. Selected bond distances (Å): Ni1−O1, 1.846(2); Ni1−N1, 1.885(2); C3−O1, 1.332(3); N1−C2, 1.426(3); N1−C8, 1.283(4). Selected bond angles (deg): O1−Ni−O1a, 180.0; N1−Ni−N1a, 180.0; O1−Ni−N1a, 93.62(9); O1−Ni−N1, 86.38(9).

The similar spectral feature at 310 nm observed during the titration of Cydo with $Zn(CH_3CO_2)_2 \cdot 2H_2O$ and $Ni(CH_3CO_2)_2 \cdot 4H_2O$ is attributed to the formation of zine in both cases. This product is the result of a ring closure reaction of Cydo. The increase in the yield of $[Ni(zine)_2]$ when Et_3N is added is attributed to the ability of Et_3N to deprotonate the phenolic OH of zine for subsequent complexation with nickel. Complexation to the metal appears to stabilize zine from ring contraction to zole.

Reactivity of Cydo with Zinc(II) Requires Acetate or Et_3N. In addition to using $Zn(CH_3CO_2)_2$, $ZnSO_4$ and $ZnCl_2$ were also used as sources of Zn^{II}. The first five spectra of Figure 5 show that the addition of 1 equiv of $ZnSO_4$ results in very minor changes to the spectrum of Cydo. A low-intensity shoulder at 320 nm appears to grow with each subsequent addition of the metal, but these subtle changes are in stark contrast to those observed for $Zn(CH_3CO_2)_2$ (see Figure 2). A significant spectral change is observed only when Et_3N is added to the Cydo/$ZnSO_4$ reaction mixture. As shown in Figure 5, adding this base results in a new absorption band at 310 nm accompanied by an isosbestic point at 300 nm, similar to the shift observed during the titration of Cydo with $Zn(CH_3CO_2)_2$ and $Ni(CH_3CO_2)_2$ and indicative of benzothiazine formation. Unlike those reactions, however, in this case the 310 nm band shifts to 320 nm,

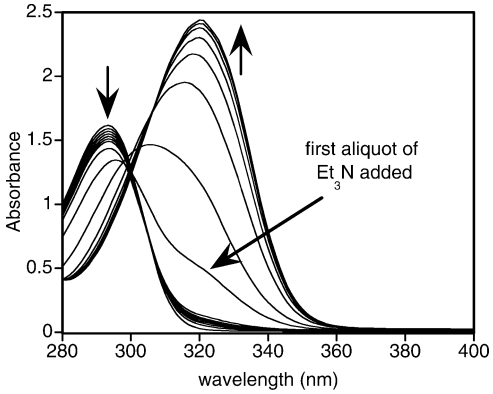

Figure 5. UV spectra of 0.62 mM Cydo in methanol at 25 °C upon the addition of up to 1 equiv of $ZnSO_4$ (first five spectra), followed by the addition of 2 equiv of Et_3N. The final spectrum, with $\lambda_{max} = 320$ nm, is consistent with the formation of a Zn−zine complex. Similar spectra were observed when $ZnCl_2$ was used.

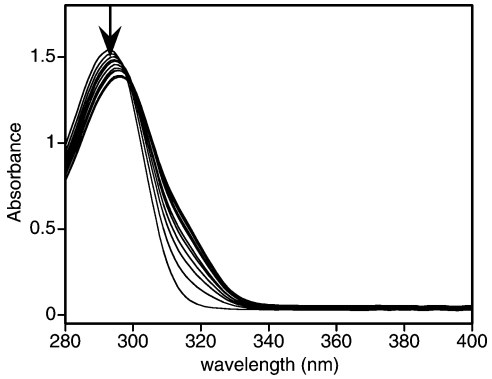

Figure 6. UV-spectrophotometric titration of 0.62 mM Cydo with a solution of $NaCH_3CO_2$ in methanol at 25 °C. Little change was observed after 12 h. Similar results were obtained when Et_3N was used in place of $NaCH_3CO_2$.

possibly indicating the formation of a Zn−zine complex. Nearly identical results were obtained for $ZnCl_2$ (data not shown).

In order to differentiate the roles of the Zn^{II} ion vs that of either Et_3N or acetate, the reactivity of Cydo with triethylamine and sodium acetate in the absence of metal ion was examined under aerobic conditions and the progress of the reaction was followed spectrophotometrically. Both additives provide indistinguishable results; therefore, only the data from the reaction with sodium acetate are shown in Figure 6. The spectra change slightly upon addition of base, with a shoulder growing in around 320 nm. The solutions change from colorless to very pale yellow overnight, although the spectra change little over this time course. These subtle changes and the pale yellow coloration suggest some conversion of Cydo to the zine and zole cyclized products, although to a much lesser extent than in the presence of Zn^{II}. Indeed, neither of these products was observed when aliquots taken from the reaction mixture were analyzed by ESI-MS. The only species detected in these mixtures by ESI-MS was the intact starting material Cydo. These results demonstrate the critical role of the metal cation in promoting the transformation of Cydo into cyclized products.

Reactivity of Cydo with Iron(III). The results of the titration of Cydo with $FeCl_3 \cdot 6H_2O$ in methanol under aerobic

(30) Parker, D.; Davies, E. S.; Wilson, C.; McMaster, J. *Inorg. Chim. Acta* **2007**, *360*, 203−211.

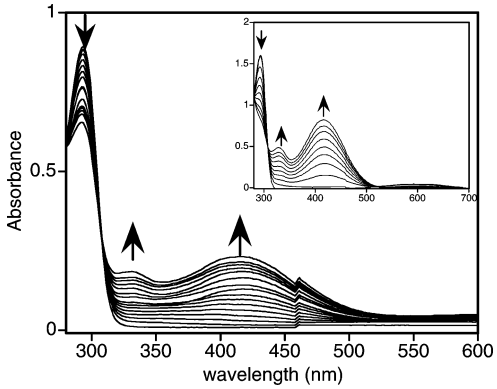

Figure 7. UV-spectrophotometric titration of 0.34 mM Cydo with 1 equiv of $FeCl_3 \cdot 6H_2O$ in methanol at 25 °C. The inset shows the UV−vis spectrophotometric titration of Cydo with $(NH_4)_2Ce(NO_3)_6$ in methanol.

conditions and ambient room temperature are shown in Figure 7. The absorption band at 293 nm due to Cydo diminishes as two new bands appear at 330 and 416 nm and the colorless methanol solution of Cydo gradually turns yellowish-green. These spectral changes are similar to what we observed previously for the titration of Cydo with $CuSO_4$ in air.[26] The 416 nm band is attributed to a two-electron oxidized *o*-quinone. This conclusion is supported by a control experiment in which the oxidation of Cydo is achieved by the common oxidizing agent ceric ammonium nitrate $(NH_4)_2Ce(NO_3)_6$. As shown by the inset in Figure 7, the oxidation of Cydo by ceric ammonium nitrate or Fe^{III} in air provides nearly identical spectral changes where the absorption band at 293 nm due to Cydo is gradually replaced by two new absorption bands at 330 and 416 nm and the colorless solution of Cydo turns yellow.

The addition of Et_3N to the Fe/Cydo reaction mixture immediately causes a drastic color change to dark purple along with the formation of a considerable amount of dark precipitate. The distinct color change is indicative of complex formation; unfortunately, repeated attempts to crystallize the isolated powder failed to yield a homogeneous product amenable to analysis.

Reactivity of Cydo and CarboxyCydo with Copper-(II). We previously reported the structure of $[Cu(zine)_2]$ as well as the zole organic fragment and speculated that it too would be a good metal-binding ligand. By isolating zole and reacting it with Cu^{II} in the presence of Et_3N, metal complexes form immediately. When the reaction is carried out in methanol, the aldehyde group of zole converts to the acetal group of $zole_{ac}$ and the methanol solvated complex $[Cu(CH_3OH)(zole_{ac})_2]$ is obtained, as shown in Figure 8. By avoiding methanol in the reaction mixture, the aldehyde version of zole is maintained and a bis THF adduct $[Cu(THF)_2(zole)_2]$ is crystallized (see the Supporting Information). Unlike the square-planar $[Cu(zine)_2]$, the zole ligands support five- or six-coordinated Cu^{II} centers, where the axial positions are taken by solvent, either a methanol in the case of the distorted square-pyramidal $[Cu(CH_3OH)(zole_{ac})_2]$ or two THF molecules in $[Cu(THF)_2(zole)_2]$. Formation of these adducts indicates that the N/O chelating motif in zole is less electron-donating than the N/O chelating motif of zine. The longer Cu−O (1.956 and 1.947 Å) and Cu−N (1.994 and 2.005 Å)

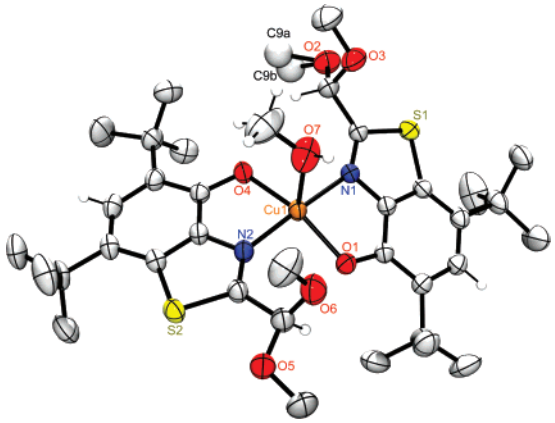

Figure 8. X-ray structure of $[Cu(CH_3OH)(zole_{ac})_2]$ showing 50% thermal ellipsoids. Selected bond distances (Å) and angles (deg): Cu1−O1, 1.947-(2); Cu1−O4, 1.956(2); Cu1−N2, 1.994(2); Cu1−N1, 2.005(2); Cu1−O7, 2.349(2); O1−Cu1−O4, 155.37(7); O1−Cu1−N2, 93.63(7); O4−Cu1−N2, 85.10(6); O1−Cu1−N1, 84.25(6); O4−Cu1−N1, 96.03(6); N2−Cu1−N1, 177.17(7); O1−Cu1−O7, 112.53(8); O4−Cu1−O7, 92.09(7); N2−Cu1−O7, 92.93(8); N1−Cu1−O7, 89.62(8).

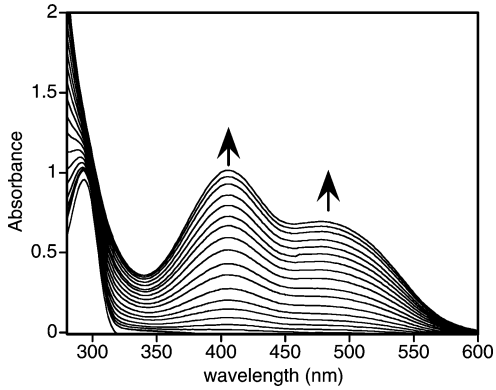

Figure 9. UV-spectrophotometric titration of 0.47 mM CarboxyCydo with 2 equiv of $CuSO_4 \cdot 5H_2O$ in methanol at 25 °C.

bond lengths of $[Cu(CH_3OH)(zole_{ac})_2]$ compared with those of $[Cu(zine)_2]$ (1.894 Å for Cu−O and 1.964 for Cu−N) also bear out this conclusion.

In order to develop an analogue to 5-*S*-cysteinyldopa closer than Cydo, we prepared CarboxyCydo, which contains a carboxylic acid group. Figure 9 shows the spectral changes resulting from the titration of a methanol solution of CarboxyCydo with 2 equiv of $CuSO_4$ under aerobic conditions and ambient room temperature. The absorption band at 293 nm due to CarboxyCydo diminishes and is accompanied by two new absorption bands at 408 and 490 nm. The solution becomes yellow during the titration. While the reactions of $CuSO_4$ with both Cydo and CarboxyCydo result in an absorption band at 408 nm,[26] attributable to the *o*-quinone, only CarboxyCydo has this second absorption band at 490 nm.

ESI-MS analysis of the reaction mixture detected two major molecular ion peaks at *m*/*z* of 306 and 338 corresponding to zole and its acetal derivative $zole_{ac}$, respectively. A molecular ion peak for 1,4-benzothiazine-3-carboxylic acid (*m*/*z* = 322) was also detected. The presence of these species, however, does not provide an explanation for the absorption band at 490 nm. In order to identify the component that gives rise to this new feature at 490 nm, the reaction mixture was

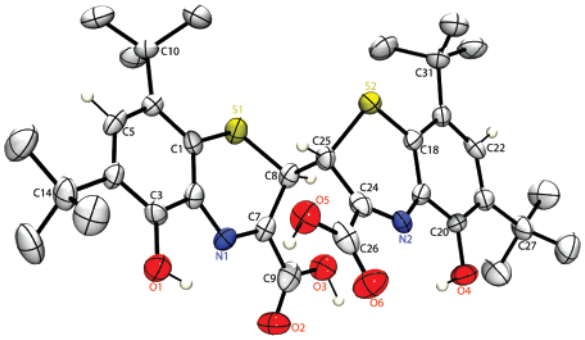

Figure 10. X-ray structure of bi-zine showing 50% thermal ellipsoids. Selected bond distances (Å): O1−C3, 1.362(5); C9−O2, 1.270(6); C2−N1, 1.403(6); C9−O3, 1.255(6); C7−N1, 1.285(6); C1−C2, 1.409(6); C1−S1, 1.766(5); C8−C7, 1.499(7); C8−S1, 1.798(4); C8−C25, 1.536(6). Selected bond angles (deg): C2−N1−C7, 121.1(4); S1−C8−C7, 107.5-(3); C1−S1−C8, 99.7(2); N1−C7−C9, 116.3(5); S1−C8−C25, 114.0(3); C2−C1−S1, 117.7(4); C8−C7−C9, 118.9(5).

evaporated to dryness and redissolved in acetonitrile. Slow evaporation of the resulting dark brown residue provided a limited amount of orange crystals that were analyzed by X-ray crystallography to reveal the 2,2′-bibenzothiazine (bi-zine) product shown in Figure 10.

In an attempt to isolate Cu complexes of the CarboxyCydo ligand, the reactions were repeated in the presence of Et_3N. The dark brown precipitate from the methanol reaction mixture was crystallized from THF by the slow diffusion of methanol. X-ray crystallographic analysis revealed the product to be the same [Cu(zine)$_2$] complex that is also obtained from the analogous reaction with Cydo. This result shows that CarboxyCydo undergoes transformations identical to those observed for Cydo, namely, a Cu-mediated oxidation to the corresponding *o*-quinone followed by formation of zine that gets trapped as the Cu^{II} complex in the presence of base. Furthermore, the isolation of [Cu(zine)$_2$] from CarboxyCydo demonstrates that the 1,4-benzothiazine-3-carboxylic acid intermediate decarboxylates to the corresponding zine to form [Cu(zine)$_2$].

Discussion

The catechol, thioether, amine, and carboxylic acid functional groups found in cysteinyldopas are all capable of interacting with metal ions, leading to a rich array of possible coordination complexes. These groups can also be reactive, especially upon oxidation, leading to cyclized intermediates that are found in red pheomelanin pigments and that may also interact with metal ions. As model compounds, Cydo and CarboxyCydo retain this unique combination of potential metal-ligating groups. We previously reported that all three types of donor atoms in Cydo simultaneously coordinate to Cu^{II} in the absence of dioxygen to form a stable, tetranuclear [Cu_4Cydo$_4$] complex, but that in the presence of oxygen and copper, Cydo converts to benzothiazine that either binds the metal to form [Cu(zine)$_2$] or further transforms to benzothiazole. In this report, we show that Zn^{II}, Ni^{II}, and Fe^{III} induce similar transformations depending on reaction conditions.

Scheme 1 summarizes the results and highlights the variety of isolated products, all of which are consistent with species implicated in the biosynthetic pathway of pheomelanin. In our system, no significant changes in the absorption spectrum of Cydo are observed upon mixing with $ZnCl_2$ or $ZnSO_4$, whereas mixing with $Zn(CH_3CO_2)_2$ induces the rapid formation of benzothiazine with a characteristic absorption feature at 310 nm. The acetate presumably acts as a base to facilitate an interaction between the metal and Cydo, which then rapidly cyclizes in air to form benzothiazine. Although we never isolated a Cydo−Zn species, a tetranuclear Cu_4Cydo_4 species forms under anaerobic conditions. The zine species can either coordinate to Zn^{II} if there is sufficient base to give a suspected Zn−zine complex with $\lambda_{max} = 320$ nm or it further rearranges into benzothiazole. The acetate anion is not a strong enough base to form a Zn(zine)$_2$ complex, but addition of Et_3N to these reaction mixtures appears to stabilize zine, suggesting that it is coordinated to Zn. This conclusion is based on the similarity observed when $Ni(CH_3CO_2)_2$ is used and the [Ni(zine)$_2$] complex is isolated.

The results with $Zn(CH_3CO_2)_2$ and $Ni(CH_3CO_2)_2$ are in stark contrast to those obtained by exposing Cydo to either $Na(CH_3CO_2)$ or Et_3N, where only subtle spectral changes are observed over the same time frame, confirming that neither the acetate anion nor Et_3N alone are responsible for the Cydo transformation to cyclized products and that the divalent metal ions play a critical role in the transformation. A previous report found that Zn promotes the aerial oxidation of cysteinyldopa while Ni, Al, Pb, and Hg do not,[19] which conflicts with the results obtained here for Ni. It should be noted that the nonreactive metal ions in that study included chloride, nitrate, or sulfate counteranions, while the source of Zn was zinc acetate. Combined, these results highlight the non-innocence of the counteranion used in studying metal−ligand interactions.

In contrast to Zn^{II}, the redox-active metal ions Cu^{II} and Fe^{III} do not require acetate to induce the aerial oxidation of Cydo or CarboxyCydo. In these cases, chloride salts of the metal ions were used, and immediately upon mixing a peak at 416 nm characteristic of an *o*-quinone appears. This peak is not observed in the Zn and Ni cases, suggesting that Cu and Fe stabilize the quinone intermediate. Cysteinyldopa quinones have been previously observed in the biomimetic reaction pathway of pheomelanin.[2,3,31] On the basis of published mechanisms, the quinone cyclizes to transient quinonimine species (not directly observed in our studies) that rearrange to benzothiazine. The instability of benzothiazines is well reported,[2] but we find that coordination to divalent metal ions stabilizes them as M(zine)$_2$ complexes.

Coordination of zine to the metal requires deprotonation of the phenolic OH, which in our system is provided by Et_3N. In the absence of a suitable base, these species undergo ring contraction to form stable benzothiazoles, a crystal structure of which we have previously reported.[26] While others have reported the formation of benzothiazoles from copper- and iron-assisted oxidations of 5-cysteinyldopa,[1] our results show that the thiazole species can also form in the presence of zinc and nickel. Stability constants of 4-hydroxybenzothia-

(31) Napolitano, A.; Memoli, S.; Crescenzi, O.; Prota, G. *J. Org. Chem.* **1996**, *61*, 598−604.

Scheme 1

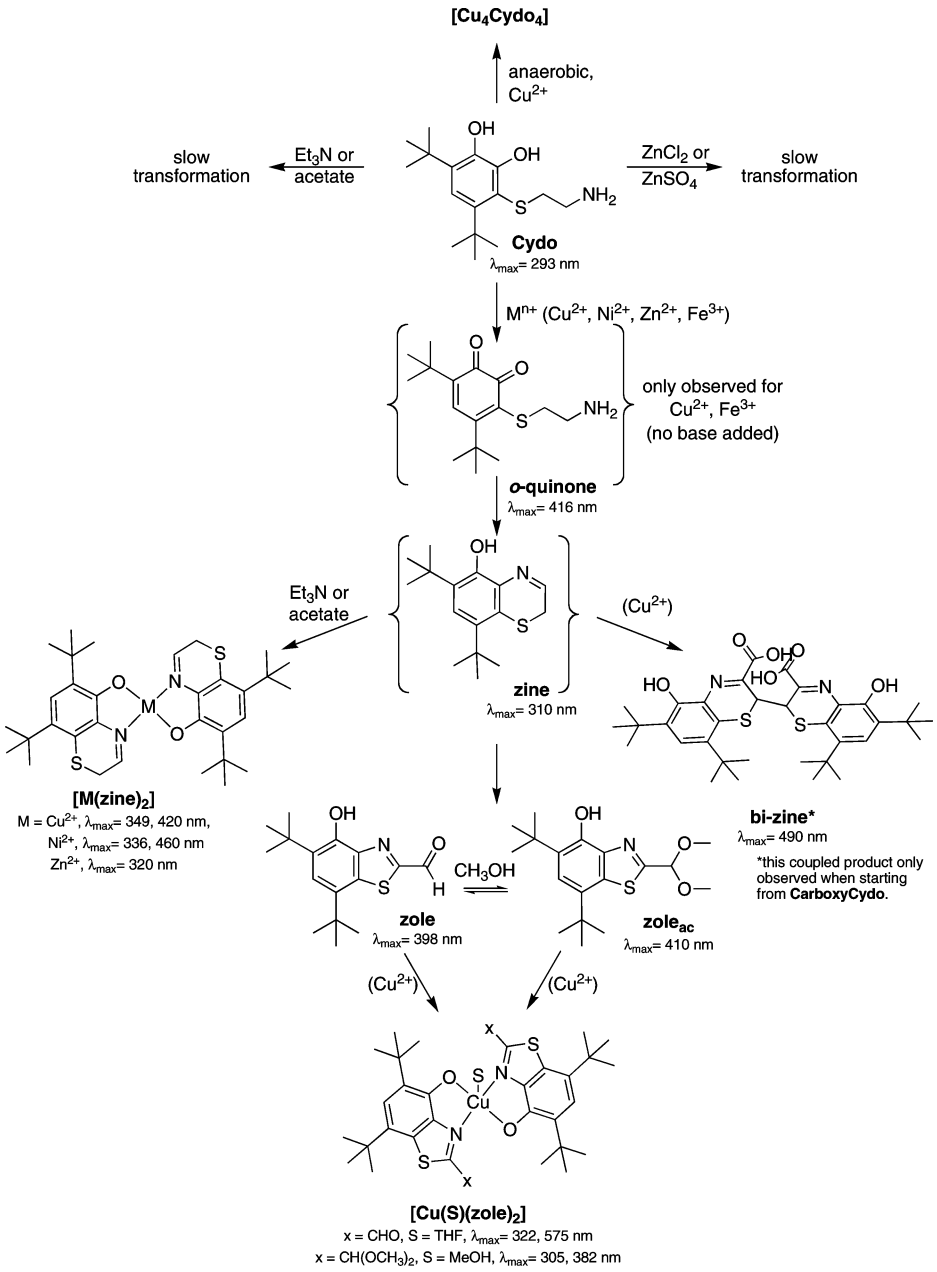

zoles, which are weaker than the more common 8-hydroxyquinoline chelating agent,[32−34] have been reported for a variety of metal ions, but surprisingly only one crystal structure of a metal complex with this chelating motif is currently known in the Cambridge Structural Database.[35] The structures reported here of $[Cu(CH_3OH)(zole_{ac})_2]$ and $[Cu(THF)_2(zole)_2]$ are the first crystallographically characterized copper complexes of hydroxybenzothiazoles and their isolation validates that these motifs, which are present in pheomelanin, are capable of binding metal ions.

In the case of CarboxyCydo, a 3-carboxy derivative of zine initially forms. However, isolation of high yields of $[Cu(zine)_2]$ from reactions of CarboxyCydo, Cu^{II}, and Et_3N suggests that this benzothiazine readily decarboxylates prior to binding Cu. In contrast, if no base is included in the reaction mixture, a unique feature appears in the absorption spectrum at 490 nm. Several species are present in this reaction mixture, including benzothiazoles and 3-carboxybenzothiazines, but the new feature giving rise to the bright orange color is attributed to bi-zine, a benzothiazine dimer that retains the carboxyl groups at the 3 position, as evidenced by its crystal structure.

These results are significant because the ratio of carboxylated vs noncarboxylated benzothiazines has been postulated to affect the reaction pathway and final components of red hair pigments.[2,36] For example, in vitro biomimetic studies

(32) Feng, P. K.; Fernando, Q. *Inorg. Chem.* **1962**, *1*, 426−427.
(33) Feng, P. K.; Fernando, Q. *J. Am. Chem. Soc.* **1960**, *82*, 2115−2118.
(34) Lane, T. J.; Lane, C. S. C.; Sam, A. *J. Am. Chem. Soc.* **1961**, *83*, 2223−2225.
(35) Perez-Lourido, P.; Romero, J.; Garcia-Vazquez, J. A.; Sousa, A.; McAuliffe, C. A.; Helliwell, M. *Inorg. Chim. Acta* **1998**, *279*, 249−251.

found that oxidation of 5-cysteinyldopa with chemical or enzymatic oxidants yielded oligomers resembling pheomelanin in which predominantly noncarboxylated benzothiazine and benzothiazole units are linked by C−C or C−O bonds.[31] In contrast, the presence of Zn^{II} during the chemical oxidation of 5-cysteinyldopa was found to divert the reaction toward the assembly of bibenzothiazines wherein carboxy-benzothiazine units dimerize at the 2 position.[18] The dimers were subsequently converted by aerial oxidation to trichochrome C, the most abundant trichochrome isolated from red hair.[18] The current results are the first to show that bibenzothiazines also result from the reaction of copper with cysteinyldopa-like molecules.

Collectively, our results emphasize the complexity of the reaction pathways available to cysteinyldopa-like species depending on the reaction conditions. The type of metal ion as well as its counteranion influence both the reaction and its products. In addition, the ability of cyclized benzothiazine units to coordinate metal ions depends on the availability of a suitable base to deprotonate the phenol for metal binding. This observation suggests that the in vivo pH of the pheomelanogenesis environment, which is not known and may deviate from 7.4, will have a critical role in the outcome of the pigment since coordination to metals can stabilize benzothiazines. When not stabilized by coordination to metal ions, benzothiazines in our system convert to either benzothiazoles, which themselves are suitable metal-binding ligands, or carboxylated bibenzothiazine.

Acknowledgment. We thank Duke University for support.

Supporting Information Available: ORTEP diagram and X-ray crystallographic information for $[Cu(THF)_2(zole)_2]$. X-ray crystallographic data, in CIF format, for $[Cydo{\cdot}HCl]{\cdot}H_2O$, (bi-zine)·$Et_2O{\cdot}2(H_2O)$, $[Ni(zine)_2]$, $[Cu(CH_3OH)(zole_{ac})_2]$, and $[Cu(THF)_2(zole)_2]$. This material is available free of charge via the Internet at http://pubs.acs.org.

IC701889W

(36) Napolitano, A.; Di Donato, P.; Prota, G. *Biochim. Biophys. Acta* **2000**, *1475*, 47−54.